NO. 2344

VISUAL OBSERVATIONS IN AN AMMONIA EVAPORATOR

M. M. SHAH

It is generally agreed that visual observations are of much value in understanding the physical phenomena that occur in evaporators. While several such studies on R-11, R-12, and R-22 evaporators have been reported, no such efforts seem to have been devoted to ammonia evaporators. Ammonia differs markedly from other common refrigerants because it is practically insoluble in oil, while R-11, R-22, and R-12 are soluble. For this reason, results of visual studies on these refrigerants are not directly applicable to ammonia evaporators.

Extensive studies on a recirculation type ammonia evaporator were made by the author at the Institute of Refrigeration, Technical University of Norway at Trondheim, Norway. In these experiments, local heat transfer coefficients and local pressure drop rates were measured, and simultaneous observations through sight glasses were made. Correlations developed from these data for predicting heat transfer and pressure drop rates are presented in another paper (1). In that paper, visual observations are discussed only briefly.

In this study, flow pattern data from several test runs are presented along with the measured heat transfer and pressure drop rates to examine any possible interrelation. The development of flow patterns along the length of the evaporator for various mass flow rates and heat fluxes is described with other phenomena like tube wetting, film climbing, etc. Flow pattern data are compared with two correlations, resulting in maps that can be used for predicting flow patterns. The behavior of oil observed in the sight glasses and its apparent effect on heat transfer and pressure drop are discussed.

EXPERIMENTAL SETUP

The experimental apparatus has already been described in Ref. 1 and is shown schematically in Fig. 1. The 140-meter long horizontal evaporator was fabricated from commerical grade steel pipe of 26.2 mm ID. The length was divided into 12 sections: the first 10.6 m long and the rest 11.77 m long. Thus, 13 stations for measuring local heat transfer and pressure drop rates were formed. Sight glasses 50 mm long, 26.2 mm ID were provided at the last 12 stations, there being no sight glass at station 0. The sight glasses were protected by perspex shields, the heating cables passing through the annular space between shield and sight glass without actually touching the latter. The last 3 sight glasses were later removed because of frequent breakages at low mass flow rates.

The ammonia compressors were of conventional reciprocating design with standard oil separators in their discharge lines. No devices for measuring or controlling the amount of oil in circulation were provided. The evaporator was frequently drained of oil. In no instance were any extraordinary amounts of oil discovered. Mobil Oil Corporation's Artic 300 oil was used in the compressors. The kinematic viscosity of this oil varies from 5000 centistoke at 0 C to 300,000 Centistokes at -30 C. The thermal conductivity of oil rises linearly from .1095 at 40 C to .113 kcal/mhr C at -17.5 C.

Tests were conducted with mass flow rates from 60 to 3000 kg/hr, heat fluxes up to 2000 kcal/m^2hr, ammonia temperatures between 0 to -40 C, and vapor qualities from 0 to 100 percent.

Details of pressure, temperature measurements, and data reduction techniques are of limited

M. M. Shah, Devon, PA

+ ASHRAE TRANS. vol. 81, part 1, 1975

NO. 2344

VISUAL OBSERVATIONS IN AN AMMONIA EVAPORATOR

M. M. SHAH

It is generally agreed that visual observations are of much value in understanding the physical phenomena that occur in evaporators. While several such studies on R-11, R-12, and R-22 evaporators have been reported, no such efforts seem to have been devoted to ammonia evaporators. Ammonia differs markedly from other common refrigerants because it is practically insoluble in oil, while R-11, R-22, and R-12 are soluble. For this reason, results of visual studies on these refrigerants are not directly applicable to ammonia evaporators.

Extensive studies on a recirculation type ammonia evaporator were made by the author at the Institute of Refrigeration, Technical University of Norway at Trondheim, Norway. In these experiments, local heat transfer coefficients and local pressure drop rates were measured, and simultaneous observations through sight glasses were made. Correlations developed from these data for predicting heat transfer and pressure drop rates are presented in another paper (1). In that paper, visual observations are discussed only briefly.

In this study, flow pattern data from several test runs are presented along with the measured heat transfer and pressure drop rates to examine any possible interrelation. The development of flow patterns along the length of the evaporator for various mass flow rates and heat fluxes is described with other phenomena like tube wetting, film climbing, etc. Flow pattern data are compared with two correlations, resulting in maps that can be used for predicting flow patterns. The behavior of oil observed in the sight glasses and its apparent effect on heat transfer and pressure drop are discussed.

EXPERIMENTAL SETUP

The experimental apparatus has already been described in Ref. 1 and is shown schematically in Fig. 1. The 140-meter long horizontal evaporator was fabricated from commerical grade steel pipe of 26.2 mm ID. The length was divided into 12 sections: the first 10.6 m long and the rest 11.77 m long. Thus, 13 stations for measuring local heat transfer and pressure drop rates were formed. Sight glasses 50 mm long, 26.2 mm ID were provided at the last 12 stations, there being no sight glass at station 0. The sight glasses were protected by perspex shields, the heating cables passing through the annular space between shield and sight glass without actually touching the latter. The last 3 sight glasses were later removed because of frequent breakages at low mass flow rates.

The ammonia compressors were of conventional reciprocating design with standard oil separators in their discharge lines. No devices for measuring or controlling the amount of oil in circulation were provided. The evaporator was frequently drained of oil. In no instance were any extraordinary amounts of oil discovered. Mobil Oil Corporation's Artic 300 oil was used in the compressors. The kinematic viscosity of this oil varies from 5000 centistoke at 0 C to 300,000 Centistokes at -30 C. The thermal conductivity of oil rises linearly from .1095 at 40 C to .113 kcal/mhr C at -17.5 C.

Tests were conducted with mass flow rates from 60 to 3000 kg/hr, heat fluxes up to 2000 $kcal/m^2hr$, ammonia temperatures between 0 to -40 C, and vapor qualities from 0 to 100 percent.

Details of pressure, temperature measurements, and data reduction techniques are of limited

M. M. Shah, Devon, PA

+ ASHRAE TRANS. vol. 81, part 1, 1975

interest for the purpose of this paper and can be found in Ref 1. Results of a heat leakage calibration test are shown in Fig. 2. It is apparent that heat leakage, calculated as the difference between the change in enthalpy of ammonia and electric heat input, is neglegibly small.

FLOW PATTERNS

Concept and Utility

The concept of flow patterns is an attempt to describe the geometry of flow. Observations indicate that the various flow geometries can be divided into a few broad classes. Various correlations have been proposed for predicting the flow patterns.

The knowledge of prevalent flow pattern has generally been utilized in two ways. One approach has been to regard it as a similarity parameter or correlating device. Thus, it is asserted that for the same flow pattern, the same approximate emperical laws govern the momentum fields in all two-phase pipe flows. This approach has been used to much success by several workers including Baker (2) who gives different correlations for different flow patterns to calculate pressure drop.

A second use is found through more fundamental considerations. If the velocity field in any flow is completely known, in principle it becomes possible to calculate the temperature and pressure distribution by the application of laws of motion and thermodynamics. The knowledge of flow pattern type is helpful to some extent in determining the velocity distribution. For example, if the flow pattern is known to be perfectly annular, pressure drop calculations become possible through the use of the Universal Velocity Distribution Law. Examples of such derivations can be found in several texts including that by Collier (6). Such approaches are of great value in obtaining a deep insight into the two-phase phenomena, but calculations based on these methods are generally cumbersome. Predictions are not necessarily accurate because flow patterns are rarely perfect, and the various assumptions made in analysis are of limited validity.

Classification

The terminology used to describe flow patterns has varied considerably with various workers. The definitions used in analysing our data are as follows:

Stratified - Liquid and vapor phases completely separated by a smooth and calm interface.

Wavy - Liquid separated on the bottom with a wavy interface. Occasional large waves or slugs may occur, but the top should remain dry most of the time.

Slug - An extension of wavy flow pattern. The frequency of slugs is greater so that the top portion of the pipe remains wet most of the time.

Crescent - Basically annular but the liquid film is noticeably thicker at the bottom. The top 1/8 may occasionally be dry.

Semi-Crescent - Basically crescent but more than the top 1/8 remains dry all the time.

Annular - An apparently uniform liquid layer covers the entire pipe circumference.

Semi-Annular - Basically annular but the top of the tube is not wet. The definitions given above are generally in agreement with the most common usage with the exception of the term semi-annular.

Data

Flow pattern data from 7 test runs are presented in Fig. 3 to 6. In Fig. 3, flow patterns and pressure drops with coil exit temperatures at approximately -30 C are shown. The development of flow patterns at 4 different mass flow rates can thus be studied together with their possible influence on pressure drop rates. In Fig. 4, the heat transfer data from the same tests are given. Fig. 5 and 6 provide similar data from coil exit temperatures around -5 C. During all these test runs the heat flux was approximately 2000 kcal/m^{2}hr.

In interpreting these data, it must be noted that the pressure drop data are raw i.e. no

interest for the purpose of this paper and can be found in Ref 1. Results of a heat leakage calibration test are shown in Fig. 2. It is apparent that heat leakage, calculated as the difference between the change in enthalpy of ammonia and electric heat input, is negligibly small.

FLOW PATTERNS

Concept and Utility

The concept of flow patterns is an attempt to describe the geometry of flow. Observations indicate that the various flow geometries can be divided into a few broad classes. Various correlations have been proposed for predicting the flow patterns.

The knowledge of prevalent flow pattern has generally been utilized in two ways. One approach has been to regard it as a similarity parameter or correlating device. Thus, it is asserted that for the same flow pattern, the same approximate emperical laws govern the momentum fields in all two-phase pipe flows. This approach has been used to much success by several workers including Baker (2) who gives different correlations for different flow patterns to calculate pressure drop.

A second use is found through more fundamental considerations. If the velocity field in any flow is completely known, in principle it becomes possible to calculate the temperature and pressure distribution by the application of laws of motion and thermodynamics. The knowledge of flow pattern type is helpful to some extent in determining the velocity distribution. For example, if the flow pattern is known to be perfectly annular, pressure drop calculations become possible through the use of the Universal Velocity Distribution Law. Examples of such derivations can be found in several texts including that by Collier (6). Such approaches are of great value in obtaining a deep insight into the two-phase phenomena, but calculations based on these methods are generally cumbersome. Predictions are not necessarily accurate because flow patterns are rarely perfect, and the various assumptions made in analysis are of limited validity.

Classification

The terminology used to describe flow patterns has varied considerably with various workers. The definitions used in analysing our data are as follows:

Stratified - Liquid and vapor phases completely separated by a smooth and calm interface.

Wavy - Liquid separated on the bottom with a wavy interface. Occasional large waves or slugs may occur, but the top should remain dry most of the time.

Slug - An extension of wavy flow pattern. The frequency of slugs is greater so that the top portion of the pipe remains wet most of the time.

Crescent - Basically annular but the liquid film is noticeably thicker at the bottom. The top 1/8 may occasionally be dry.

Semi-Crescent - Basically crescent but more than the top 1/8 remains dry all the time.

Annular - An apparently uniform liquid layer covers the entire pipe circumference.

Semi-Annular - Basically annular but the top of the tube is not wet. The definitions given above are generally in agreement with the most common usage with the exception of the term semi-annular.

Data

Flow pattern data from 7 test runs are presented in Fig. 3 to 6. In Fig. 3, flow patterns and pressure drops with coil exit temperatures at approximately -30 C are shown. The development of flow patterns at 4 different mass flow rates can thus be studied together with their possible influence on pressure drop rates. In Fig. 4, the heat transfer data from the same tests are given. Fig. 5 and 6 provide similar data from coil exit temperatures around -5 C. During all these test runs the heat flux was approximately 2000 kcal/m^{2}hr.

In interpreting these data, it must be noted that the pressure drop data are raw i.e. no

curve smoothing has been done. The heat transfer coefficients have been obtained from smoothed out curves of mean wall temperatures as explained in Ref 1.

Analysis of Data

All flow pattern observations were made with the naked eye, and no photographs were taken. The transition from one flow pattern to another was gradual, and it was often difficult to decide in which class the observed pattern should be placed. Distinguishing between slug and wavy, and crescent and annular flows was specially difficult. Perfectly stratified flow was never observed, a few disturbing waves being always present in even the quietest interface. Occasionally, the flow pattern was such as could not be placed in any well defined class. No attempt was made to correlate such odd observations. Finally, the analyses to follow include the data in Fig. 3 to 6 as well as all the other data not included in these figures.

The development of flow patterns generally followed the behavior described in the texts and in published studies on other evaporators. This is evident from Fig. 3 to 6. At moderate flow rates, boiling started with mildly wavy flow. With increasing vapor quality, the waves became more frequent and larger in amplitude until the flow could definitely be called slug. Further down the length, the slugs became lass frequent and violent and the liquid began to climb up the walls in a film. With increasing vapor quality, crescent flow developed, and further down the length, annular flow occured.

At the highest mass flow rates, wavy flow was eliminated, the flow going directly from all liquid to slug, to crescent, and then to annular. At the lowest flow rates, slug flow was rare. The boiling region commenced with mildly wavy flow, became more wavy, and then tended to crescent and annular patterns. At temperatures around -5 C and low mass flow rates, liquid film did not climb up the walls sufficiently to cover the whole pipe circumference. Thus under these conditions, only semi-crescent and semi-annular patterns could develop. In general, the higher the evaporating temperature, the more the circumference of the pipe was left dry. At high mass flow rates, most of the pipe circumference was always wet at all evaporating temperatures.

All the flow pattern observations noted in the foregoing may be generalized to state that with increasing vapor velocity, liquid tends to form into a film around the pipe circumference. The higher the vapor velocity, the greater the extent of wetted perimeter will be. Higher vapor velocity results from high total mass flow rate, high vapor quality, and low ammonia temperature.

Study of Fig. 3 to 6 reveals that the peak of heat transfer and pressure drop occurs somewhere between 85 and 90% vapor qualities. This is in agreement with observations of other refrigerant evaporators, like Chawla's experiments on R-11 (7). Very few observations in the liquid deficiency region could be made because sight glasses broke frequently under these conditions. Only one test with liquid deficiency conditions in which visual observations were made could be satisfactorily completed. The coil exit saturation temperature in that test was -15 C. As the peak of heat transfer was passed, the thin annular liquid film became discontinuous, and thus, part of pipe circumference became dry. Furthermore, wall and ammonia temperatures showed a slow cyclic variation at vapor qualities higher than approximately 80%.

In Fig. 3 and 5 at the lowest mass flow rates, the interrelation between pressure drop and flow pattern seems apparent. The slope of the curve changes markedly as flow pattern varies from wavy to semi-crescent. The effect of temperature is also marked. The pressure drop at -30 C is seen to be roughly twice the pressure drop at -5 C. Definite conclusions regarding interrelation of heat transfer with flow pattern and evaporating temperature cannot be drawn because of the approximate nature of the heat transfer data.

Baker Correlation

The best known correlation for predicting flow patterns is that by Baker (2). The parameters used are dimensional, and hence, the various terms are defined in the following along with their units:

ρ_g = Density of vapor, lb/ft^3

ρ_l = Density of liquid, lb/ft^3

curve smoothing has been done. The heat transfer coefficients have been obtained from smoothed out curves of mean wall temperatures as explained in Ref 1.

Analysis of Data

All flow pattern observations were made with the naked eye, and no photographs were taken. The transition from one flow pattern to another was gradual, and it was often difficult to decide in which class the observed pattern should be placed. Distinguishing between slug and wavy, and crescent and annular flows was specially difficult. Perfectly stratified flow was never observed, a few disturbing waves being always present in even the quietest interface. Occasionally, the flow pattern was such as could not be placed in any well defined class. No attempt was made to correlate such odd observations. Finally, the analyses to follow include the data in Fig. 3 to 6 as well as all the other data not included in these figures.

The development of flow patterns generally followed the behavior described in the texts and in published studies on other evaporators. This is evident from Fig. 3 to 6. At moderate flow rates, boiling started with mildly wavy flow. With increasing vapor quality, the waves became more frequent and larger in amplitude until the flow could definitely be called slug. Further down the length, the slugs became lass frequent and violent and the liquid began to climb up the walls in a film. With increasing vapor quality, crescent flow developed, and further down the length, annular flow occured.

At the highest mass flow rates, wavy flow was eliminated, the flow going directly from all liquid to slug, to crescent, and then to annular. At the lowest flow rates, slug flow was rare. The boiling region commenced with mildly wavy flow, became more wavy, and then tended to crescent and annular patterns. At temperatures around -5 C and low mass flow rates, liquid film did not climb up the walls sufficiently to cover the whole pipe circumference. Thus under these conditions, only semi-crescent and semi-annular patterns could develop. In general, the higher the evaporating temperature, the more the circumference of the pipe was left dry. At high mass flow rates, most of the pipe circumference was always wet at all evaporating temperatures.

All the flow pattern observations noted in the foregoing may be generalized to state that with increasing vapor velocity, liquid tends to form into a film around the pipe circumference. The higher the vapor velocity, the greater the extent of wetted perimeter will be. Higher vapor velocity results from high total mass flow rate, high vapor quality, and low ammonia temperature.

Study of Fig. 3 to 6 reveals that the peak of heat transfer and pressure drop occurs somewhere between 85 and 90% vapor qualities. This is in agreement with observations of other refrigerant evaporators, like Chawla's experiments on R-11 (7). Very few observations in the liquid deficiency region could be made because sight glasses broke frequently under these conditions. Only one test with liquid deficiency conditions in which visual observations were made could be satisfactorily completed. The coil exit saturation temperature in that test was -15 C. As the peak of heat transfer was passed, the thin annular liquid film became discontinuous, and thus, part of pipe circumference became dry. Furthermore, wall and ammonia temperatures showed a slow cyclic variation at vapor qualities higher than approximately 80%.

In Fig. 3 and 5 at the lowest mass flow rates, the interrelation between pressure drop and flow pattern seems apparent. The slope of the curve changes markedly as flow pattern varies from wavy to semi-crescent. The effect of temperature is also marked. The pressure drop at -30 C is seen to be roughly twice the pressure drop at -5 C. Definite conclusions regarding interrelation of heat transfer with flow pattern and evaporating temperature cannot be drawn because of the approximate nature of the heat transfer data.

Baker Correlation

The best known correlation for predicting flow patterns is that by Baker (2). The parameters used are dimensional, and hence, the various terms are defined in the following along with their units:

ρ_g = Density of vapor, lb/ft^3

ρ_l = Density of liquid, lb/ft^3

$\lambda = [(\rho_g/.075)(\rho_l/62.3)]^{1/2}$

μ_l = Liquid viscosity, Centipoise

ν = Surface tension of liquid, dynes per cm

$\beta = (73/\nu)[\mu_l(62.3/\rho_l)^2]^{1/3}$

G_g = Mass flux of gas phase based on total cross-section of pipe, lb/ft^{2}hr

G_l = Mass flux of liquid phase based on total cross-section of pipe, lb/ft^{2}hr

The abscissa on Baker's chart is $(G_l\lambda\beta/G_g)$, while the ordinate is (G_g/λ).

The results of the calculations according to this method are shown in Fig . 7. The dashed lines and designations in quotes are according to Baker. The firm lines and designations are according to the author's data. Baker does not specifically define crescent, semi-crescent, or semi-annular regimes. These must, therefore, be considered part of the region designated by him as annular. Allowing for some inevitable overlapping at boundries between different regimes, it is seen that the agreement is quite good. Essentially, our data has served to provide a more detailed map of the area designated as annular in the standard Baker chart. Knowledge of these details is of practical significance. Because of the large differences in thermal conductivity of vapors and liquids, heat transfer rate for a partially wet surface is likely to be significantly lower than if the whole surface is wet. Thus, other things being the same, heat transfer coefficients for the semi-annular regime will be expected to be lower than in the annular regime.

The only apparent discrepancy is in the wavy regime. None of our data points fall in the area provided for it in Baker's chart but instead fall on a narrow strip at the borders of stratified, slug, and annular regimes. Noting that the stratified, wavy, and slug regimes differ only in the intensity and frequency of distrubances and that wavy and slug flows transform gradually into annular flow, the location of wavy data on the map is not surprising.

Griffith and Wallis Correlation

Griffith and Wallis (3) proposed a correlation which was really intended for locating the boundries of slug regime for flow in vertical pipes. The correlation is simple and non-dimensional. The abscissa is the Froude number (Fr) given by:

$$Fr = [(Q_l+Q_g)/A]^2/g.D \qquad (1)$$

where:

Q_l and Q_g are volume flow rates of the liquid and gas phases respectively.

A is the cross-sectional area of the pipe,

D is its diameter and

g is the acceleration due to gravity.

The ordinate is the vapor volume fraction $[Q_g/(Q_l+Q_g)]$.

Fig. 8 and 9 show the representation of our ammonia data with this correlation. The various flow regimes are well separated and it appears likely that this map could be used to predict flow patterns in other ammonia evaporators.

BEHAVIOR OF OIL

Oil was observed in the evaporator in many of the tests. The observations in the boiling and non-boiling regions are discussed separately in the following.

Non-boiling Region

The effect of oil in the non-boiling region (all liquid flow) was most pronounced in some tests carried out at high mass flow rates and low temperatures. Thick oil films were seen around the circumference of sight glasses. Sometimes the oil films were stationary, and some-

$\lambda = [(\rho_g/.075)(\rho_l/62.3)]^{1/2}$

μ_l = Liquid viscosity, Centipoise

ν = Surface tension of liquid, dynes per cm

$\beta = (73/\nu)[\mu_l(62.3/\rho_l)^2]^{1/3}$

G_g = Mass flux of gas phase based on total cross-section of pipe, lb/ft^{2}hr

G_l = Mass flux of liquid phase based on total cross-section of pipe, lb/ft^{2}hr

The abscissa on Baker's chart is $(G_l\lambda\beta/G_g)$, while the ordinate is (G_g/λ).

The results of the calculations according to this method are shown in Fig . 7. The dashed lines and designations in quotes are according to Baker. The firm lines and designations are according to the author's data. Baker does not specifically define crescent, semi-crescent, or semi-annular regimes. These must, therefore, be considered part of the region designated by him as annular. Allowing for some inevitable overlapping at boundries between different regimes, it is seen that the agreement is quite good. Essentially, our data has served to provide a more detailed map of the area designated as annular in the standard Baker chart. Knowledge of these details is of practical significance. Because of the large differences in thermal conductivity of vapors and liquids, heat transfer rate for a partially wet surface is likely to be significantly lower than if the whole surface is wet. Thus, other things being the same, heat transfer coefficients for the semi-annular regime will be expected to be lower than in the annular regime.

The only apparent discrepancy is in the wavy regime. None of our data points fall in the area provided for it in Baker's chart but instead fall on a narrow strip at the borders of stratified, slug, and annular regimes. Noting that the stratified, wavy, and slug regimes differ only in the intensity and frequency of distrubances and that wavy and slug flows transform gradually into annular flow, the location of wavy data on the map is not surprising.

Griffith and Wallis Correlation

Griffith and Wallis (3) proposed a correlation which was really intended for locating the boundries of slug regime for flow in vertical pipes. The correlation is simple and non-dimensional. The abscissa is the Froude number (Fr) given by:

$$Fr = [(Q_l+Q_g)/A]^2/g.D \qquad (1)$$

where:

Q_l and Q_g are volume flow rates of the liquid and gas phases respectively.

A is the cross-sectional area of the pipe,

D is its diameter and

g is the acceleration due to gravity.

The ordinate is the vapor volume fraction $[Q_g/(Q_l+Q_g)]$.

Fig. 8 and 9 show the representation of our ammonia data with this correlation. The various flow regimes are well separated and it appears likely that this map could be used to predict flow patterns in other ammonia evaporators.

BEHAVIOR OF OIL

Oil was observed in the evaporator in many of the tests. The observations in the boiling and non-boiling regions are discussed separately in the following.

Non-boiling Region

The effect of oil in the non-boiling region (all liquid flow) was most pronounced in some tests carried out at high mass flow rates and low temperatures. Thick oil films were seen around the circumference of sight glasses. Sometimes the oil films were stationary, and some-

times they moved slowly. Occasionally, the stationary oil films were seen to have a cellular structure strikingly similar in appearance to photographs of the Benard effect in stationary liquid films, e.g. Fig. 1 in Chandrashekhar's text (4). Whether or not this observation of apparently cellular structure has any significance is unknown. No conclusions from the same are attempted. When thick, apparently solid, oil films were observed, single phase heat transfer coefficients were exceptionally low while the pressure drops were exceptionally high. The low heat transfer rate is obviously caused by the thermal resistance of the oil film. High pressure drop is caused by the reduction in flow area caused by oil film and in the case of moving oil films also by the additional energy required to drag the oil film along.

Fig. 10 shows the results of such a test in which ammonia temperature varied between -34 C and -26 C. Thick oil films were seen at stations 1, 2, and 3. At the same locations, very low heat transfer coefficients and very high pressure drops were measured. After station 5, the friction factor drops down to a little below .018, while heat transfer coefficients rise to about -30% of the equation:

$$Nu = 0.1825\ Re^{0.509}\ Pr^{0.4} \qquad (2)$$

Eq(2) was presented in Ref 1 and correlated our data for single phase heat transfer coefficients within ± 30%. Here, Nu is the Nusselt number, Re is the Reynolds number, and Pr is the Prandtl number.

Continuous oil films were also sometimes observed at higher ammonia temperatures, but their influence on heat transfer and pressure drop was only moderate. Measured heat transfer coefficients were within -30% of Eq(2). This is explained by the fact that the viscosity of the oil used decreased sharply with increasing temperature, and its set point is in the vicinity of -18 C. Thus at higher temperatures, oil cannot solidify and remains at relatively low viscosity. Hence, the oil films formed cannot be very thick.

A question that may now be raised is why thick oil films were not always observed at temperatures around -30 C? Part of the explanation lies in the fact that the amount of oil varied form test to test. With less oil in circulation, the chances of film formation are less. Furthermore, as long as the oil and ammonia are well mixed and in rapid motion, the properties of the mixture will be the weighted mean of the properties of the components, and oil will not freeze out of the mixture easily. However, if oil once freezes on the surface of the pipe due to some chance circumstance, it will not normally be brought back into circulation unless heated to above its set point.

The other important problem to be faced is that even when no oil films were observed, measured heat transfer coefficients were much lower than the predicitions of the Dittus-Boelter equation. They instead satisfied Eq(2) to within ± 30%. If it is assumed that a thin oil film exists around the pipe circumference, its thickness can be calculated:

$$\frac{1}{h_m} = \frac{1}{k/\delta} + \frac{1}{h_i} \qquad (3)$$

where:

h_m is the measured heat transfer coefficient,

h_i is the heat transfer coefficient claculated by the Dittus-Boelter equation:

$$Nu = 0.023\ Re^{0.8}\ Pr^{0.4} \qquad (4)$$

Further:

k is the thermal conductivity of oil and

δ is the thickness of oil film.

Estimating h_m by Eq(2), the mean thickness of oil film was calculated and the results were shown in Fig. 6 of Ref 1. The results may also be represented by:

$$\delta/D = .028/Re^{.23} \qquad (5)$$

where:

δ is the oil film thickness

Re is the Reynolds Number of ammonia liquid

times they moved slowly. Occasionally, the stationary oil films were seen to have a cellular structure strikingly similar in appearance to photographs of the Benard effect in stationary liquid films, e.g. Fig. 1 in Chandrashekhar's text (4). Whether or not this observation of apparently cellular structure has any significance is unknown. No conclusions from the same are attempted. When thick, apparently solid, oil films were observed, single phase heat transfer coefficients were exceptionally low while the pressure drops were exceptionally high. The low heat transfer rate is obviously caused by the thermal resistance of the oil film. High pressure drop is caused by the reduction in flow area caused by oil film and in the case of moving oil films also by the additional energy required to drag the oil film along.

Fig. 10 shows the results of such a test in which ammonia temperature varied between -34 C and -26 C. Thick oil films were seen at stations 1, 2, and 3. At the same locations, very low heat transfer coefficients and very high pressure drops were measured. After station 5, the friction factor drops down to a little below .018, while heat transfer coefficients rise to about -30% of the equation:

$$Nu = 0.1825\ Re^{0.509}\ Pr^{0.4} \qquad (2)$$

Eq(2) was presented in Ref 1 and correlated our data for single phase heat transfer coefficients within $\pm$ 30%. Here, Nu is the Nusselt number, Re is the Reynolds number, and Pr is the Prandtl number.

Continuous oil films were also sometimes observed at higher ammonia temperatures, but their influence on heat transfer and pressure drop was only moderate. Measured heat transfer coefficients were within -30% of Eq(2). This is explained by the fact that the viscosity of the oil used decreased sharply with increasing temperature, and its set point is in the vicinity of -18 C. Thus at higher temperatures, oil cannot solidify and remains at relatively low viscosity. Hence, the oil films formed cannot be very thick.

A question that may now be raised is why thick oil films were not always observed at temperatures around -30 C? Part of the explanation lies in the fact that the amount of oil varied form test to test. With less oil in circulation, the chances of film formation are less. Furthermore, as long as the oil and ammonia are well mixed and in rapid motion, the properties of the mixture will be the weighted mean of the properties of the components, and oil will not freeze out of the mixture easily. However, if oil once freezes on the surface of the pipe due to some chance circumstance, it will not normally be brought back into circulation unless heated to above its set point.

The other important problem to be faced is that even when no oil films were observed, measured heat transfer coefficients were much lower than the predicitions of the Dittus-Boelter equation. They instead satisfied Eq(2) to within $\pm$ 30%. If it is assumed that a thin oil film exists around the pipe circumference, its thickness can be calculated:

$$\frac{1}{h_m} = \frac{1}{k/\delta} + \frac{1}{h_i} \qquad (3)$$

where:

h_m is the measured heat transfer coefficient,

h_i is the heat transfer coefficient claculated by the Dittus-Boelter equation:

$$Nu = 0.023\ Re^{0.8}\ Pr^{0.4} \qquad (4)$$

Further:

k is the thermal conductivity of oil and

δ is the thickness of oil film.

Estimating h_m by Eq(2), the mean thickness of oil film was calculated and the results were shown in Fig. 6 of Ref 1. The results may also be represented by:

$$\delta/D = .028/Re^{.23} \qquad (5)$$

where:

δ is the oil film thickness

Re is the Reynolds Number of ammonia liquid

D is the diameter of pipe

In the range of experimentation, Eq(5) yields oil film thicknesses from .04 mm to .11 mm. As the oil used was almost colorless, it is quite possible that thin oil films might have escaped observation. Thus, the hypothesis that thin insulating oil films are formed in ammonia evaporators must be considered as quite likely to be true though they must await final confirmation through appropriately conducted experiments. Belief in such a hypothesis has, however, been expressed by some authors. As an example, Handbuch Der Kältetechnikk (5) compares the heat transfer data for oil-free and oil containing evaporators. The heat transfer coefficients for oil containing evaporators are noted to be lower, and it is suggested that this is caused by formation of oil films on heat transfer surface.

It is of interest to study the results obtained during an analogous test program conducted by R. Grønnerud on the same test apparatus but using R-12 (8). Analysis of his single phase heat transfer data showed good argeement with the predictions of the Dittus-Boelter equation. With R-12, being completely miscible with oil, no insulating oil films are to be expected. This agreement provides reassurance as to the reliability of the test apparatus and thus in the reliability of the results obtained with ammonia as the test fluid.

Boiling Region

In the boiling region, the thick oil films completely surrounding the pipe circumference were never seen. Generally, at the inception of boiling, a small amount of oil was noticed to be flowing slowly at the bottom of the pipe. As the vapor quality increased, oil tended to climb up the walls of the pipe as a thin film. Thus, as ammonia liquid formed an annular pattern, oil tended to form a semi-annular pattern. Oil film climbing to as much as 2/3 of the tube diameter was sometimes observed.

It is likely that very thin, invisible oil films also exist in the boiling region. However, our boiling heat transfer data are not accurate enough to permit any reliable estimates of the thickness of these alleged oil films.

EFFECT OF OIL ON MEAN HEAT TRANSFER COEFFICIENTS

An idea of the effect of variations in oil content can be obtained from Fig. 11, which shows the average heat transfer coefficients for the whole evaporator (including boiling as well as non-boiling lengths) as functions of mass flow rate; heat flux is constant at 2000 kcal/m^2hr and coil exit temperatures vary between -5 and -30 C. The mean heat transfer coefficients were calculated by numerically integrating the measured local heat transfer coefficients. When little or no oil was observed in sight glasses, oil content was considered to be normal. When substantial amounts of oil were observed, oil content was considered to be heavy.

Fig. 11 indicates that heat transfer coefficients for conditions of heavy oil concentration are about 30% lower than those for normal oil content. This suggests that the heat transfer performance of an ammonia evaporator can vary considerably depending on the effectiveness of the oil separator, the frequency of oil drainage, etc.

Some light is also thrown by Fig. 11 on the effect of evaporating temperature. At the lowest flow rates, the mean heat transfer coefficient seems to increase with decreasing temperature. This may be partly explained by greater pipe wetting observed at lower evaporating temperature when mass flow rates are low. At higher flow rates, the evaporating temperature does not appear to have any marked effect. Part of the explanation lies in the observation that surface wetting is complete at high mass flow rates at all evaporating temperatures.

Use of Fig. 11 for design purposes is by no means suggested. Calculations of local heat transfer coefficients over short elements of length provide the only reliable way to properly evaluate the effect of various significant variables.

VIBRATIONS AND PRESSURE PULSATIONS

Pressures and pressure drops, as observed on the manometers, often fluctuate. The fluctuations were most intense and rapid in the slug flow regime. No measurements of frequency or intensity of fluctuations were done. The means of the fluctuating pressures and pressure drops were noted by judgment alone. Subsequent plotting of these measured pressure drops on graphs indicated that the judgment regarding the observed mean had generally been good.

D is the diameter of pipe

In the range of experimentation, Eq(5) yields oil film thicknesses from .04 mm to .11 mm. As the oil used was almost colorless, it is quite possible that thin oil films might have escaped observation. Thus, the hypothesis that thin insulating oil films are formed in ammonia evaporators must be considered as quite likely to be true though they must await final confirmation through appropriately conducted experiments. Belief in such a hypothesis has, however, been expressed by some authors. As an example, Handbuch Der Kältetechnikk (5) compares the heat transfer data for oil-free and oil containing evaporators. The heat transfer coefficients for oil containing evaporators are noted to be lower, and it is suggested that this is caused by formation of oil films on heat transfer surface.

It is of interest to study the results obtained during an analogous test program conducted by R. Grønnerud on the same test apparatus but using R-12 (8). Analysis of his single phase heat transfer data showed good argeement with the predictions of the Dittus-Boelter equation. With R-12, being completely miscible with oil, no insulating oil films are to be expected. This agreement provides reassurance as to the reliability of the test apparatus and thus in the reliability of the results obtained with ammonia as the test fluid.

Boiling Region

In the boiling region, the thick oil films completely surrounding the pipe circumference were never seen. Generally, at the inception of boiling, a small amount of oil was noticed to be flowing slowly at the bottom of the pipe. As the vapor quality increased, oil tended to climb up the walls of the pipe as a thin film. Thus, as ammonia liquid formed an annular pattern, oil tended to form a semi-annular pattern. Oil film climbing to as much as 2/3 of the tube diameter was sometimes observed.

It is likely that very thin, invisible oil films also exist in the boiling region. However, our boiling heat transfer data are not accurate enough to permit any reliable estimates of the thickness of these alleged oil films.

EFFECT OF OIL ON MEAN HEAT TRANSFER COEFFICIENTS

An idea of the effect of variations in oil content can be obtained from Fig. 11, which shows the average heat transfer coefficients for the whole evaporator (including boiling as well as non-boiling lengths) as functions of mass flow rate; heat flux is constant at 2000 kcal/m^2hr and coil exit temperatures vary between -5 and -30 C. The mean heat transfer coefficients were calculated by numerically integrating the measured local heat transfer coefficients. When little or no oil was observed in sight glasses, oil content was considered to be normal. When substantial amounts of oil were observed, oil content was considered to be heavy.

Fig. 11 indicates that heat transfer coefficients for conditions of heavy oil concentration are about 30% lower than those for normal oil content. This suggests that the heat transfer performance of an ammonia evaporator can vary considerably depending on the effectiveness of the oil separator, the frequency of oil drainage, etc.

Some light is also thrown by Fig. 11 on the effect of evaporating temperature. At the lowest flow rates, the mean heat transfer coefficient seems to increase with decreasing temperature. This may be partly explained by greater pipe wetting observed at lower evaporating temperature when mass flow rates are low. At higher flow rates, the evaporating temperature does not appear to have any marked effect. Part of the explanation lies in the observation that surface wetting is complete at high mass flow rates at all evaporating temperatures.

Use of Fig. 11 for design purposes is by no means suggested. Calculations of local heat transfer coefficients over short elements of length provide the only reliable way to properly evaluate the effect of various significant variables.

VIBRATIONS AND PRESSURE PULSATIONS

Pressures and pressure drops, as observed on the manometers, often fluctuate. The fluctuations were most intense and rapid in the slug flow regime. No measurements of frequency or intensity of fluctuations were done. The means of the fluctuating pressures and pressure drops were noted by judgment alone. Subsequent plotting of these measured pressure drops on graphs indicated that the judgment regarding the observed mean had generally been good.

In most tests, the evaporator vibrated to some extent. In some tests, the vibrations were so intense that the whole evaporator shook violently. These vibrations are believed to have been caused by the pulsations during wavy and slug flow.

CONCLUDING REMARKS

The main objective of this paper was to describe the visual observations made during the described tests to provide an understanding of the physical phenomena occuring in the evaporator and to furnish the necessary background against which the quantitative results and correlations presented in the earlier paper (1) could be interpreted. This being the only visual study on ammonia evaporators reported until now, it is hoped that this adds some useful information.

Several methods for calculating heat transfer and pressure drop require the knowledge of flow patterns. For this purpose, Fig. 7 to 9 are useful. As the Baker correlation has been found to be successful for a wide variety of fluids and flow conditions, Fig. 7 can be recommended for predicting flow patterns with much confidence. The use of Fig. 8 and 9 should be made with caution, as the Griffith and Wallis correlation has not been verified for a wide variety of data.

The basic shortcoming of our tests has been the absence of control and measurement of oil content. While it can be inferred from the data with much confidence that oil affects the heat transfer and pressure drop profoundly, it is difficult to reach definite, reliable conclusions regarding its quantiative effects. However, it is felt that Eq(2) and Eq(5) give reasonable estimates for single phase heat transfer coefficient and oil film thickness respectively.

Most reports of research efforts end by noting the need for more research and this one is no exception. However, in view of the considerable difficulties in experimenting with ammonia and the long held belief that extinction of ammonia systems is near at hand, further experimental efforts do not seem very likely. As ammonia evaporators nevertheless persist, so does the need for pertinent information. To ease the situation, the author has tabulated and compiled some of his basic data into a booklet and would gladly send it to any interested person or institution.

REFERENCES

1. M. M. Shah, "Heat Transfer and Pressure Drop in Ammonia Evaporators," ASHRAE TRANSACTIONS 1974, Vol. 80, Part 2.

2. O. Baker, "Simultaneous Flow of Oil and Gas," Oil and Gas Journal, Vol. 53, No. 12, 1954, pp 185-190.

3. P. Griffith, and G. B. Wallis, "Two-Phase Slug Flow," Journal of Heat Transfer, Transactions of the ASME, Series C, Vol. 83, 1961, pp 307-320.

4. S. Chandrashekhar, Hydrodynamcis and Hydromagnetic Stability, Oxford University Press, London, 1961.

5. R. Plank, (ed.), Handbuch Der Kältetechnikk, Vol. 3, p 441, Springer Verlag, Karlsrühe.

6. J. G. Collier, Convective Boiling and Condensation, McGraw-Hill, London, 1972.

7. J. M. Chawla, "Local Heat Transfer and Pressure Drop for Refrigerants Evaporating in Horizontal Tubes," Proceedings of the IIR, Commission 2, Trondheim, June 1966.

8. G. Lorentzen and R. Grønnerud, "On the Design of Recirculation Type Evaporators," Kulde, No. 4, August 1967.

In most tests, the evaporator vibrated to some extent. In some tests, the vibrations were so intense that the whole evaporator shook violently. These vibrations are believed to have been caused by the pulsations during wavy and slug flow.

CONCLUDING REMARKS

The main objective of this paper was to describe the visual observations made during the described tests to provide an understanding of the physical phenomena occuring in the evaporator and to furnish the necessary background against which the quantitative results and correlations presented in the earlier paper (1) could be interpreted. This being the only visual study on ammonia evaporators reported until now, it is hoped that this adds some useful information.

Several methods for calculating heat transfer and pressure drop require the knowledge of flow patterns. For this purpose, Fig. 7 to 9 are useful. As the Baker correlation has been found to be successful for a wide variety of fluids and flow conditions, Fig. 7 can be recommended for predicting flow patterns with much confidence. The use of Fig. 8 and 9 should be made with caution, as the Griffith and Wallis correlation has not been verified for a wide variety of data.

The basic shortcoming of our tests has been the absence of control and measurement of oil content. While it can be inferred from the data with much confidence that oil affects the heat transfer and pressure drop profoundly, it is difficult to reach definite, reliable conclusions regarding its quantiative effects. However, it is felt that Eq(2) and Eq(5) give reasonable estimates for single phase heat transfer coefficient and oil film thickness respectively.

Most reports of research efforts end by noting the need for more research and this one is no exception. However, in view of the considerable difficulties in experimenting with ammonia and the long held belief that extinction of ammonia systems is near at hand, further experimental efforts do not seem very likely. As ammonia evaporators nevertheless persist, so does the need for pertinent information. To ease the situation, the author has tabulated and compiled some of his basic data into a booklet and would gladly send it to any interested person or institution.

REFERENCES

1. M. M. Shah, "Heat Transfer and Pressure Drop in Ammonia Evaporators," ASHRAE TRANSACTIONS 1974, Vol. 80, Part 2.

2. O. Baker, "Simultaneous Flow of Oil and Gas," Oil and Gas Journal, Vol. 53, No. 12, 1954, pp 185-190.

3. P. Griffith, and G. B. Wallis, "Two-Phase Slug Flow," Journal of Heat Transfer, Transactions of the ASME, Series C, Vol. 83, 1961, pp 307-320.

4. S. Chandrashekhar, Hydrodynamcis and Hydromagnetic Stability, Oxford University Press, London, 1961.

5. R. Plank, (ed.), Handbuch Der Kältetechnikk, Vol. 3, p 441, Springer Verlag, Karlsruhe.

6. J. G. Collier, Convective Boiling and Condensation, McGraw-Hill, London, 1972.

7. J. M. Chawla, "Local Heat Transfer and Pressure Drop for Refrigerants Evaporating in Horizontal Tubes," Proceedings of the IIR, Commission 2, Trondheim, June 1966.

8. G. Lorentzen and R. Grønnerud, "On the Design of Recirculation Type Evaporators," Kulde, No. 4, August 1967.

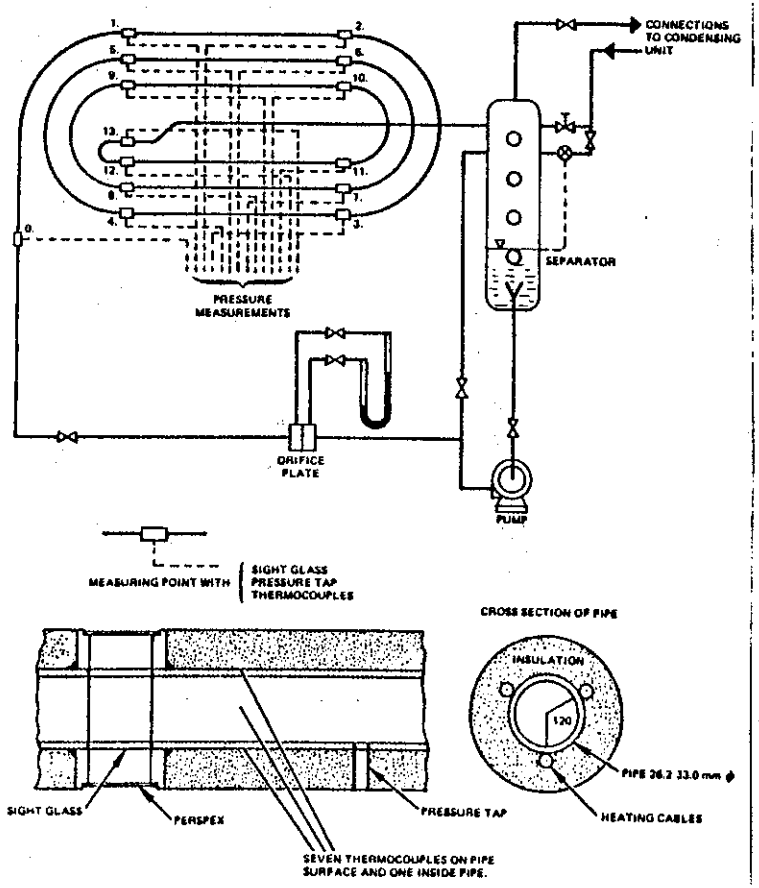

Fig. 1 Schematic arrangement and some design details of test evaporator

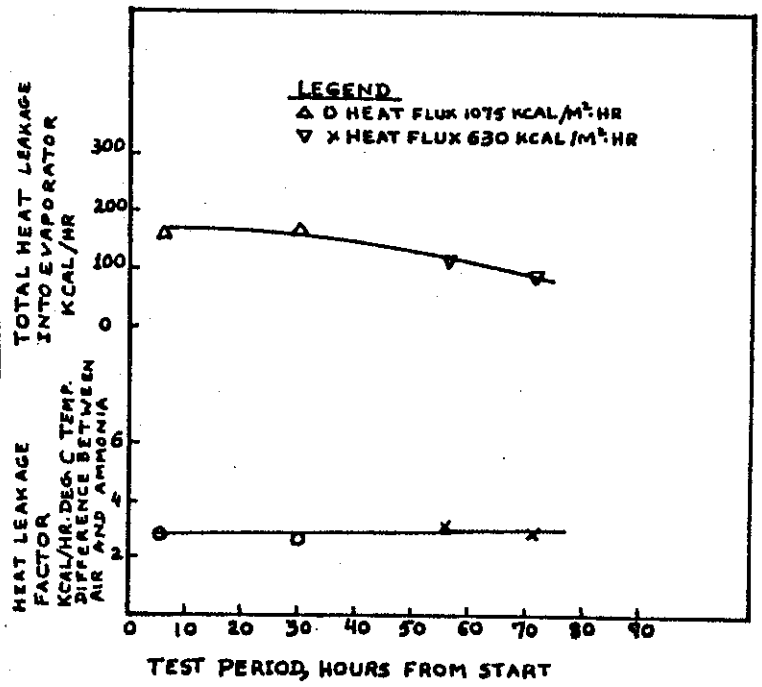

Fig. 2 Results of heat leakage calibration test. Ammonia temperature -36 to -41C. No boiling occured in evaporator.

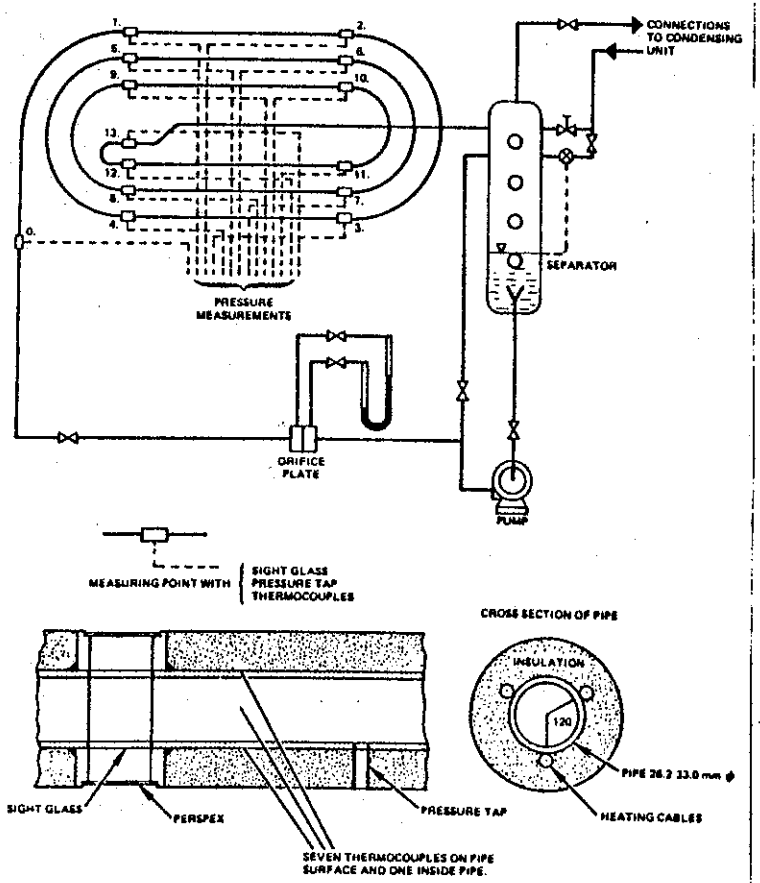

Fig. 1 Schematic arrangement and some design details of test evaporator

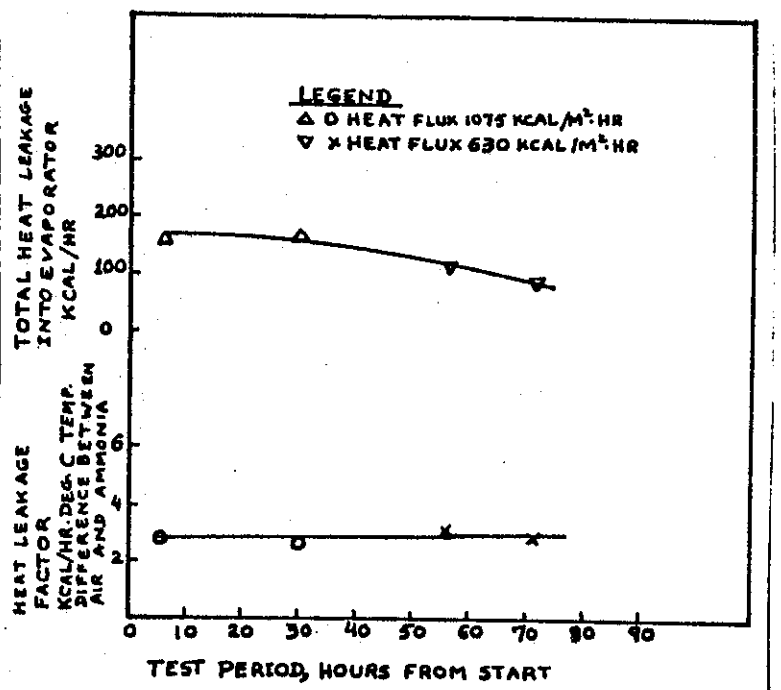

Fig. 2 Results of heat leakage calibration test. Ammonia temperature -36 to -41C. No boiling occured in evaporator.

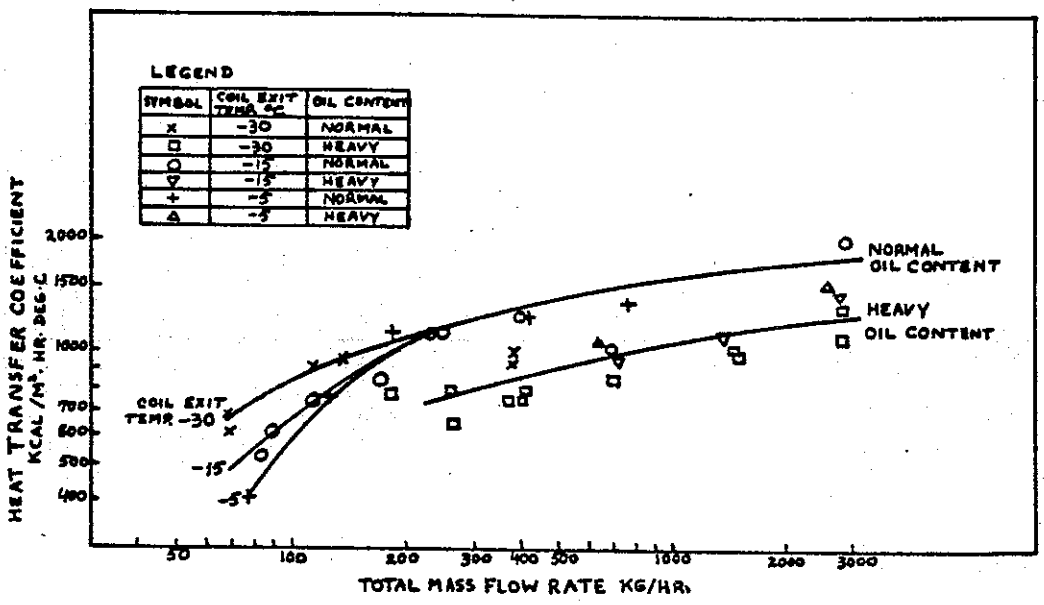

Fig. 11 Effect of mass flow rate and oil content on average heat transfer coefficients. Heat flux approximately 2000 kcal/ m^2.hr.

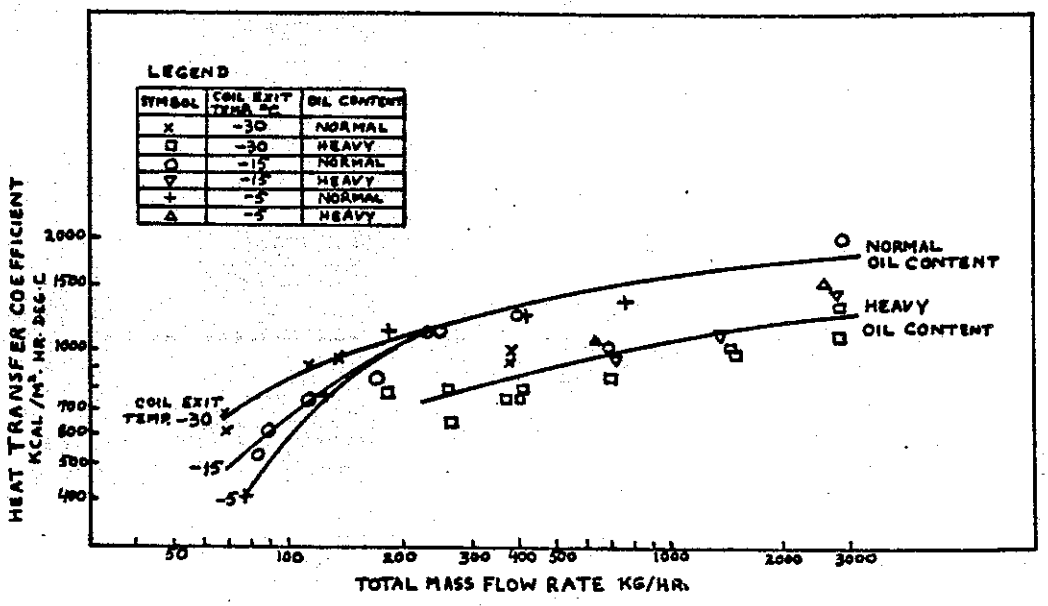

Fig. 11 Effect of mass flow rate and oil content on average heat transfer coefficients. Heat flux approximately 2000 kcal/ m².hr.

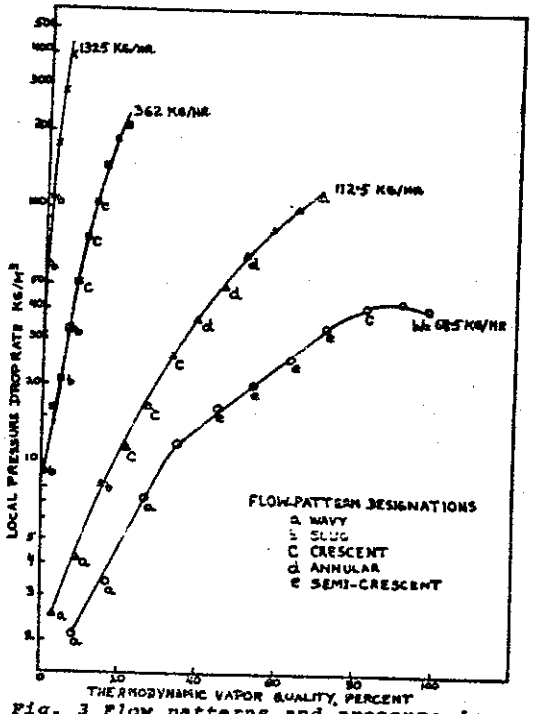

Fig. 3 Flow patterns and pressure drops as function of vapor quality and mass flow rate. Coil exit temperature approximately -30C.

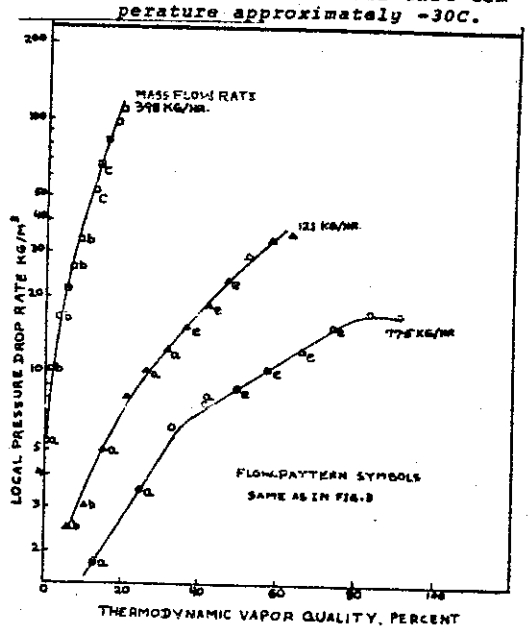

Fig. 5 Flow patterns and pressure drops as function of vapor quality and mass flow rate. Coil exit temperature approximately -5C.

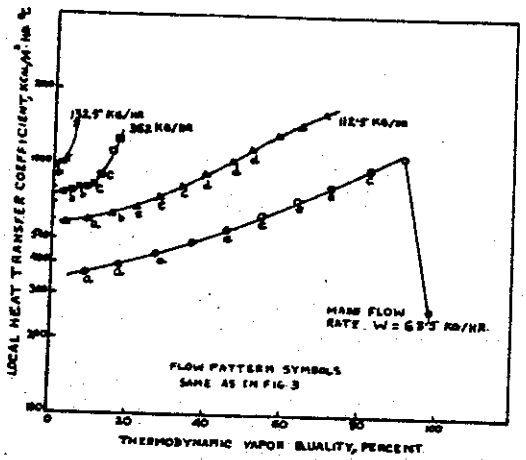

Fig. 4 Local heat transfer coefficients and flow patterns as function of mass flow rate and vapor quality. Coil exit temperature approximately -30C.

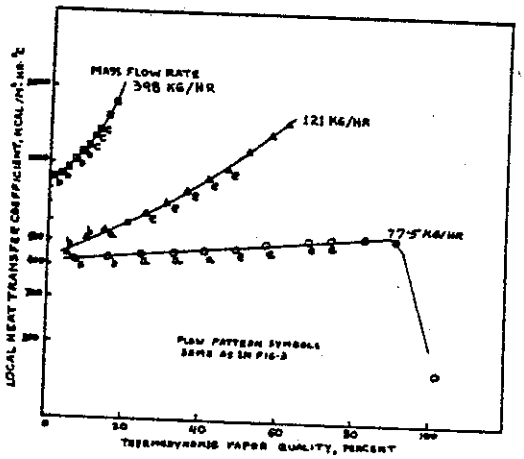

Fig. 6 Flow patterns and heat transfer coefficients as function of mass flow rate and vapor quality. Coil exit temperature approximately -5C.

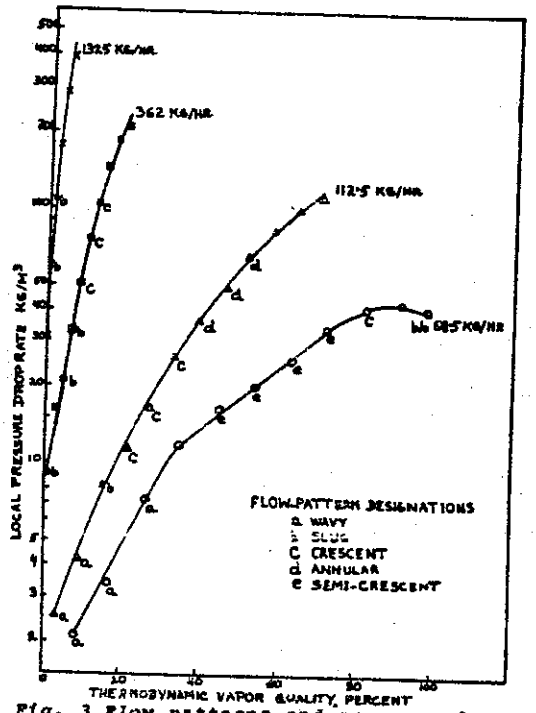

Fig. 3 Flow patterns and pressure drops as function of vapor quality and mass flow rate. Coil exit temperature approximately -30C.

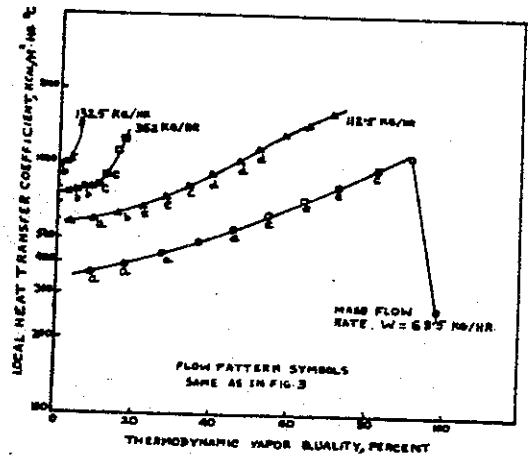

Fig. 4 Local heat transfer coefficients and flow patterns as function of mass flow rate and vapor quality. Coil exit temperature approximately -30C.

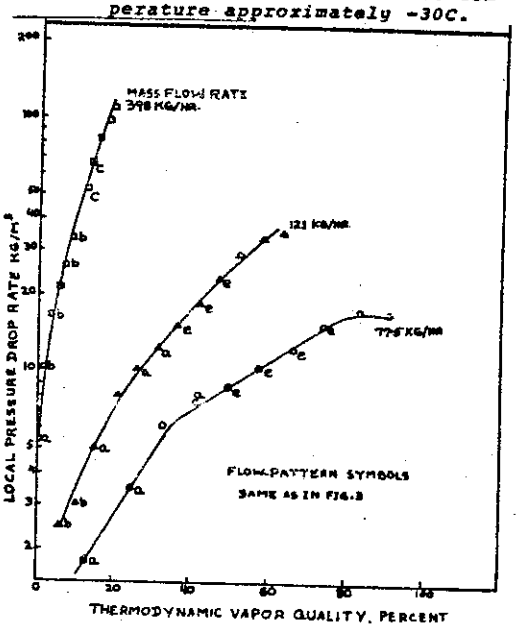

Fig. 5 Flow patterns and pressure drops as function of vapor quality and mass flow rate. Coil exit temperature approximately -5C.

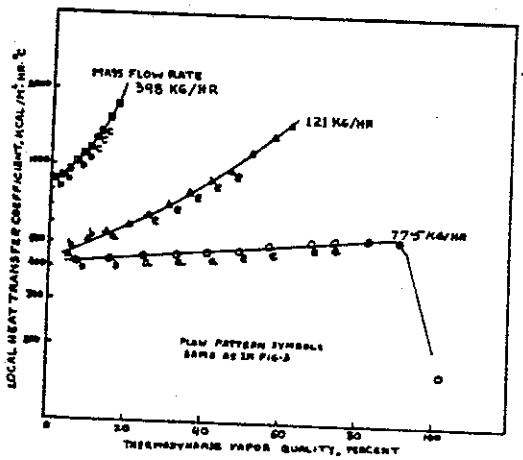

Fig. 6 Flow patterns and heat transfer coefficients as function of mass flow rate and vapor quality. Coil exit temperature approximately -5C.

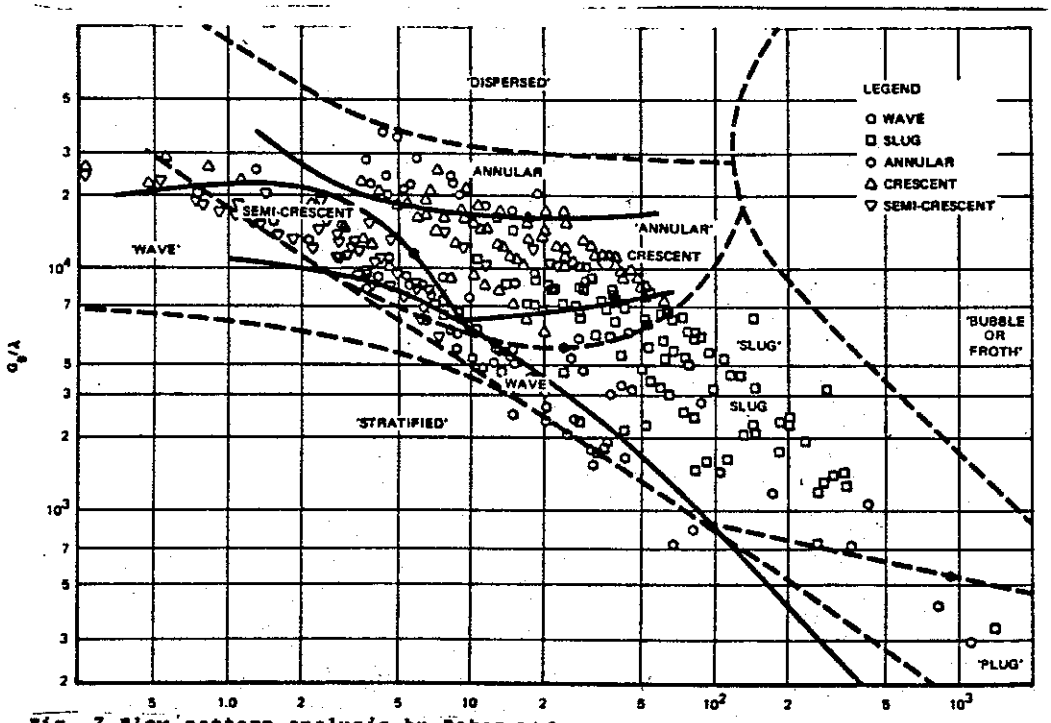

Fig. 7 Flow pattern analysis by Baker $G_l\lambda\beta/G_g$ correlation. Pattern designations in quotes and bounded by dotted lines are according to Baker.

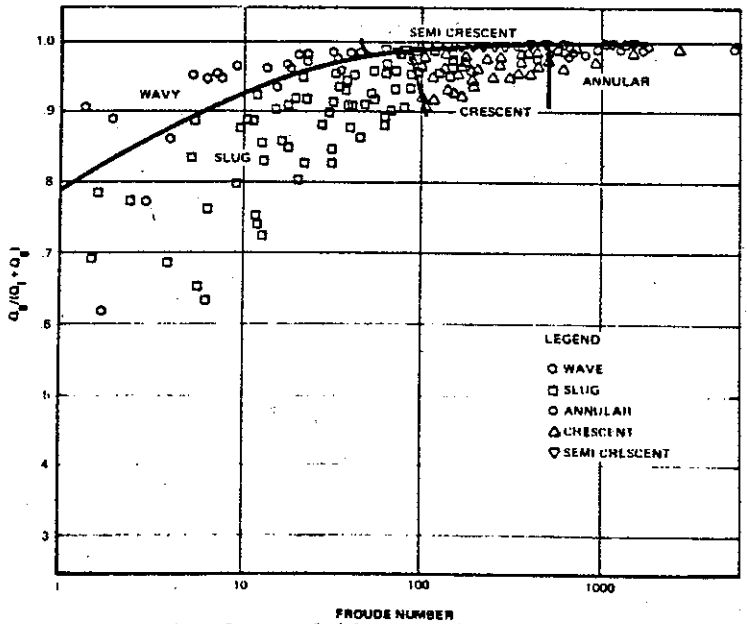

Fig. 8 Correlation of flow pattern data according to method of Griffith and Wallis

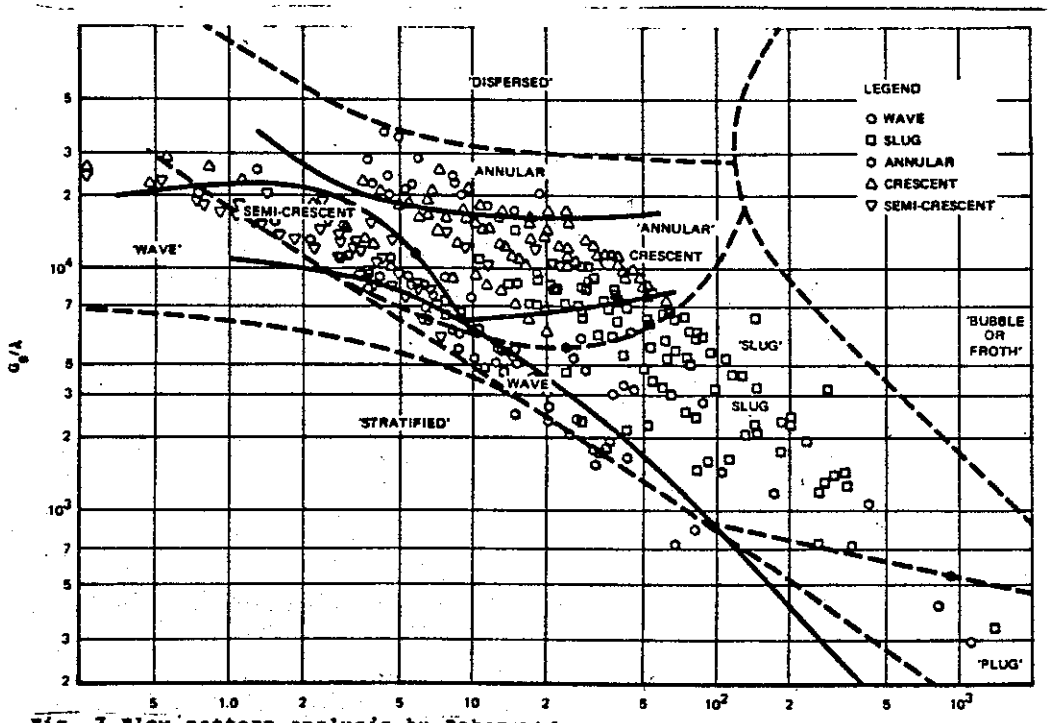

Fig. 7 Flow pattern analysis by Baker $G_l\lambda\beta/G_g$ correlation. Pattern designations in quotes and bounded by dotted lines are according to Baker.

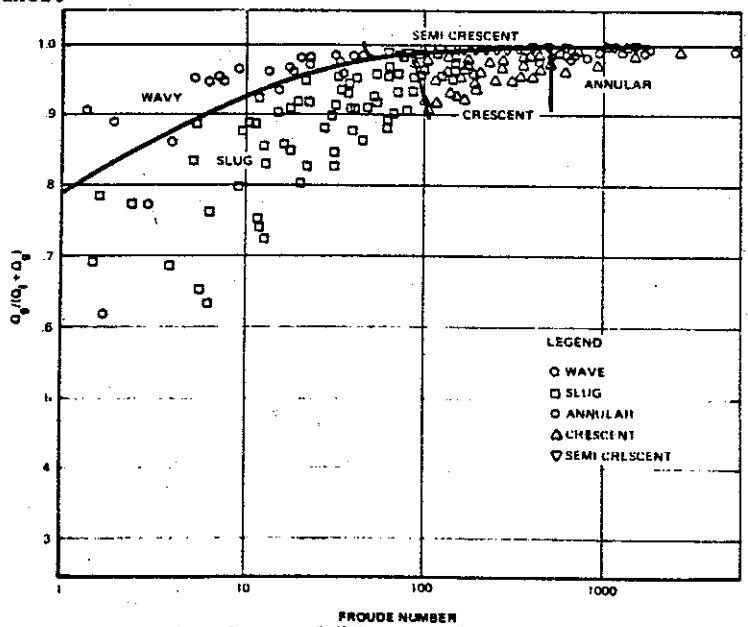

Fig. 8 Correlation of flow pattern data according to method of Griffith and Wallis

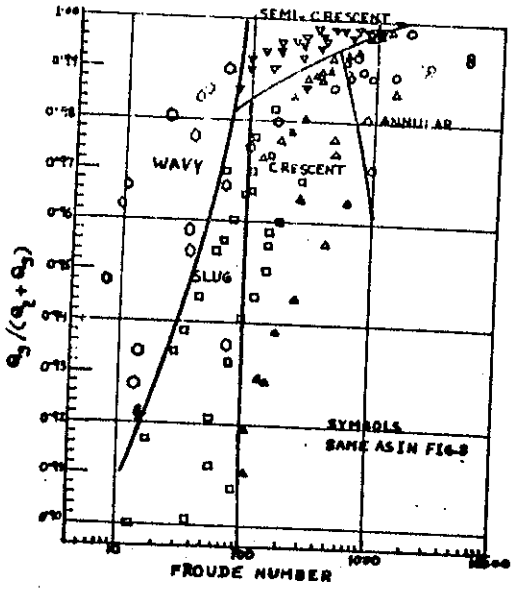

Fig. 9 Correlation of flow pattern data by method of Griffith and Wallis for ordinate between 0.9 and 1.0.

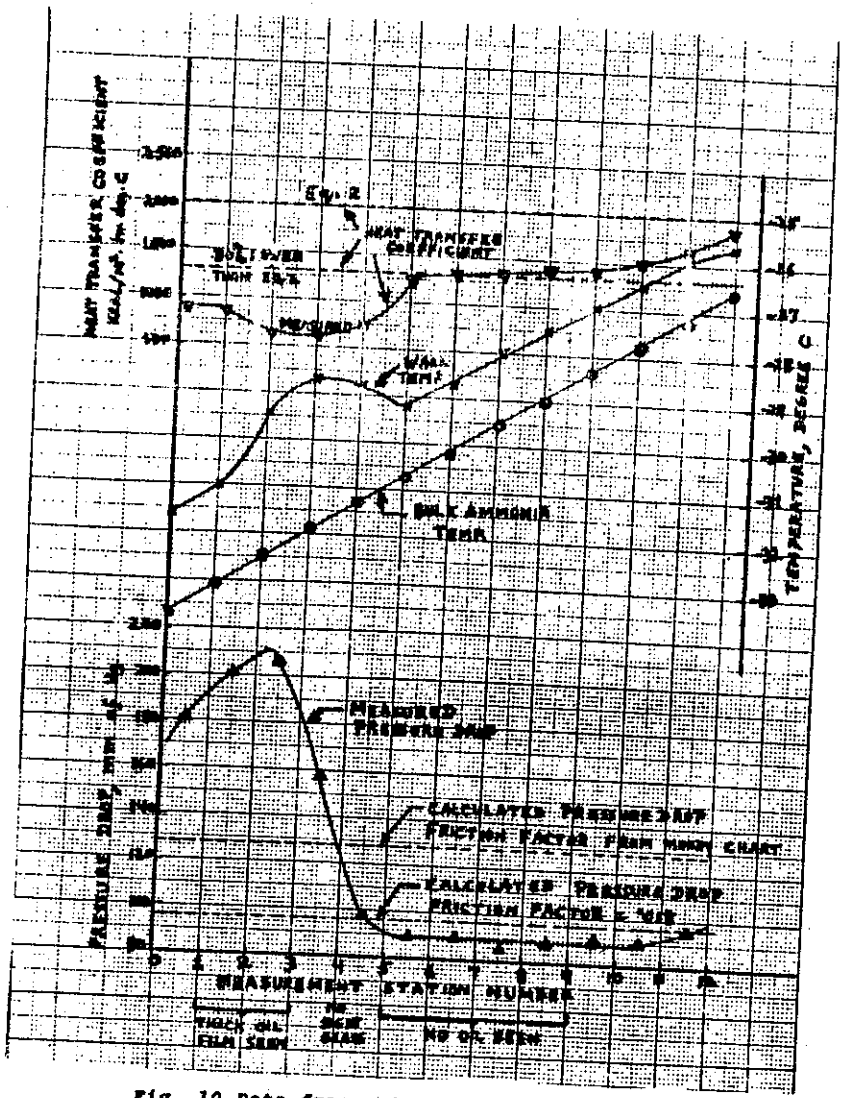

Fig. 10 Data from a test in which thick, apparently solid oil films were seen. Mass flow rate 2802 kg/hr, heat flux 2000 kcal/m^2.hr. Reynolds number 150,000

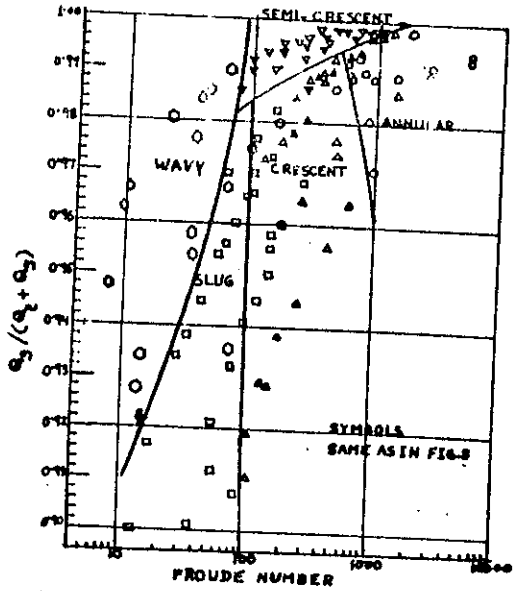

Fig. 9 Correlation of flow pattern data by method of Griffith and Wallis for ordinate between 0.9 and 1.0.

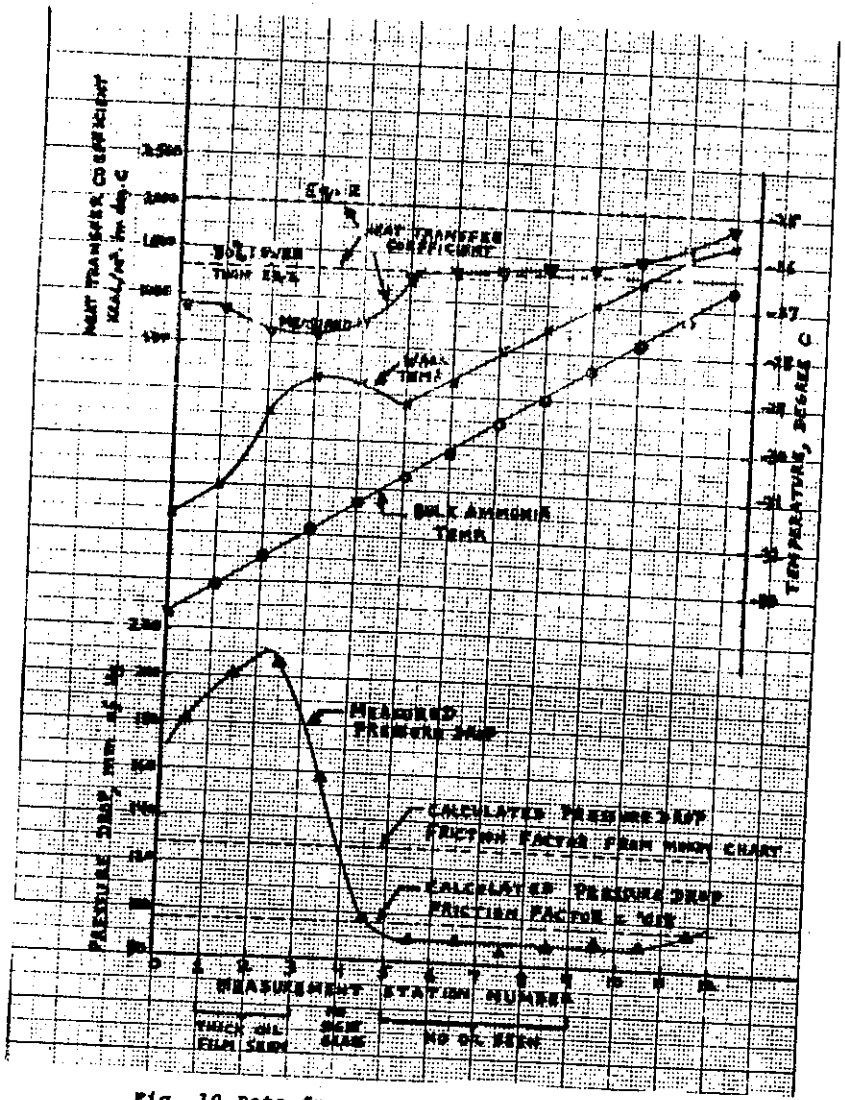

Fig. 10 Data from a test in which thick, apparently solid oil films were seen. Mass flow rate 2802 kg/hr, heat flux 2000 kcal/m^2.hr. Reynolds number 150,000